# Mesoscopic self-organization of a self-assembled supramolecular rectangle on highly oriented pyrolytic graphite and Au(111) surfaces

Jian-Ru Gong*, Li-Jun Wan*†, Qun-Hui Yuan*, Chun-Li Bai*†, Hershel Jude‡, and Peter J. Stang†‡

*Institute of Chemistry, Chinese Academy of Sciences, Beijing 100080, China; and ‡Department of Chemistry, University of Utah, 315 South 1400 East, Salt Lake City, UT 84112

Contributed by Peter J. Stang, December 8, 2004

**A self-assembled supramolecular metallacyclic rectangle was investigated with scanning tunneling microscopy on highly oriented pyrolytic graphite and Au(111) surfaces. The rectangles spontaneously adsorb on both surfaces and self-organize into well ordered adlayers. On highly oriented pyrolytic graphite, the long edge of the rectangle stands on the surface, forming a 2D molecular network. In contrast, the face of the rectangle lays flat on the Au(111) surface, forming linear chains. The structures and intramolecular features obtained through high-resolution scanning tunneling microscopy imaging are discussed.**

metallacyclic macrocycle | scanning tunneling microscopy | molecular adlayer | molecular orientation

Self-organization (1) and self-assembly (2) are critical and necessary processes in all living organisms and are of ever increasing importance in chemistry and material science. These processes will play a critical role in the so-called "bottom-up" strategy of nanofabrication. Therefore, understanding the organization of molecules on solid surfaces is important, both from a fundamental and applied perspective, for the construction of surface molecular nanostructures and nanodevices (3–13). A self-organized molecular pattern with control of structure and derived concomitant function could provide promising materials for the construction of nanodevices that cannot be prepared by conventional microfabrication. The arrangement of adsorbed molecules onto a surface depends on both intermolecular and molecule–surface interactions. For example, Hipps and colleagues (3, 4) prepared a self-organized 2D bifunctional structure on a Au(111) surface with NiTPP [nickel(II) tetraphenyl-21H,23H-porphine] and F16CoPc [colbalt(II) hexadecafluoro-29H,31H-phthalocyanine]. The two molecules are alternately aligned on the Au(111) surface and form a well defined pattern. The intermolecular interaction between NiTPP and F16CoPc plays an important role in the formation of the 2D crystalline structure. Itaya's group (5) observed different adlayers of crown-ether-substituted phthalocyanine on Au(111) and Au(100) surfaces illustrating the importance of molecule–substrate interactions. On the same gold surface the mode of crystallization results in a different self-assembly as well as different chemical reactivity in host–guest recognition. Likewise, PVBA (4-[*trans*-2-(pyrid-4-yl-vinyl)]benzoic acid) forms different adlayers on Cu(111) and Ag(111) surfaces (7).

Metal-containing macrocycles with high symmetry and precise architecture are a new class of promising supramolecules for future application in nanotechnology because of their exact shape and size, as well as magnetic, photophysical, and electrostatic properties (14–27). In this article, we describe scanning tunneling microscopy (STM) studies of the self-assembled supramolecular metallacyclic rectangle, cyclobis[(1,8-bis(transPt($PEt_3$)$_2$)anthracene)(1,4′-bis(4-ethynylpyridyl)benzene]($PF_6$)$_4$, (Fig. 1) (28). The dimensions of a single rectangle molecule were independently determined to be 3.1 nm long by 1.2 nm wide, from the previously reported x-ray crystallographic data (28). The molecular adlayers were prepared on highly oriented pyrolytic graphite (HOPG) and Au(111) surfaces to investigate the effect of substrate on adlayer formation. The molecules self-organize into well ordered 2D adlayers on both surfaces, and high-resolution STM results clearly reveal an intact rectangle on both HOPG and Au(111) surfaces, but the symmetry and molecular orientation the molecules adopt depends on the substrate.

## Materials and Methods

**Chemicals.** The $PF_6^-$ salt of the rectangle was prepared analogously to the $ClO_4^-$ salt previously reported (28), substituting $KPF_6$ for $NaClO_4$.

**Substrates.** HOPG (quality ZYB) was purchased from Digital Instruments (Santa Barbara, CA). The (111) facets on a gold single-crystal bead, prepared by melting gold wire (99.999%), were used as substrate and for the STM experiment (5, 6, 9–11). Before molecular adlayer formation, the (111) surface was quenched in hydrogen-saturated ultrapure (Milli-Q; $\geq$18.2 M$\Omega$ cm) water to obtain a clean (1 $\times$ 1) structure.

**Molecular Adlayers and STM Measurements.** Molecular adlayers of the rectangle were prepared on both HOPG and Au(111) surfaces. On HOPG the adlayer was prepared by depositing a toluene (HPLC grade, Aldrich) solution containing the rectangle (2 $\mu$l; $10^{-6}$ M) on an atomically flat surface of freshly cleaved HOPG. However, orientation of the molecular adlayer does not depend on solvent because similar images were observed when the sample was prepared from water, ethanol, or methylene chloride. After evaporation of the solvent, the STM images were recorded in the open atmosphere with a Nanoscope IIIa SPM instrument (Digital Instruments). Mechanically cut Pt/Ir wires (90/10) were used as STM tips for HOPG samples.

Molecular adlayers were prepared on the Au(111) surface by immersing the single-crystal gold bead into a $10^{-6}$ M toluene solution of the rectangle for 3–5 min, rinsing thoroughly with Milli-Q water, and mounting the resultant bead into the STM electrochemical cell. The STM images were recorded with a Nanoscope E STM instrument (Digital Instruments) in a $HClO_4$ solution prepared by diluting ultrapure $HClO_4$ (Cica-Merck, Kanto Kagaku, Japan) with Milli-Q water under potential control at the double-layer potential region. The typical potential used in these experiments was 400 mV, where no surface redox reactions take place and the molecular self-assembly is preserved. The reference and counter electrodes were platinum wires, and all potentials are reported versus the reversible hydrogen electrode in 0.1 M $HClO_4$. Because of the ease of gold

Abbreviations: HOPG, highly oriented pyrolytic graphite; STM, scanning tunneling microscopy.

†To whom correspondence may be addressed. E-mail: wanlijun@iccas.ac.cn, clbai@iccas.ac.cn, or stang@chem.utah.edu.

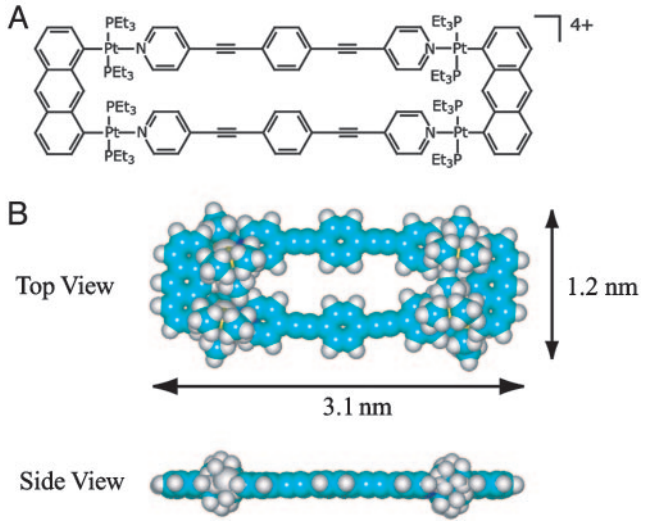


**Fig. 1.** Chemical structure (*A*) and space-filling model (*B*), from a top and side view, of the rectangle.

surface contamination in an open atmosphere, the STM experiments were preformed in solution where the electrolyte solution protects the surface from atmospheric contaminants (5, 6). The STM tips for gold samples were prepared by electrochemically etching (12–15 V) a tungsten wire (0.25 mm in diameter) in 0.6 M KOH until the etching process stopped. The tungsten tips were coated with clear nail polish to minimize Faradaic current. STM images were recorded in constant-current mode, without further processing (e.g., highpass filtering), to evaluate the corrugation heights of the adsorbed molecules. Tunneling conditions are reported in the figure legends.

## Results and Discussion

**Self-Organization on HOPG.** Solution concentration is crucial to forming a monolayer on the HOPG surface. The rectangles ($10^{-6}$ M solution in toluene) adsorb on the surface of HOPG and self-organize into a well ordered 2D molecular network. At lower concentrations only small domains of the HOPG surface were covered with the rectangle, whereas concentrations $>10^{-4}$ M result in surface clusters because of the charged character of the molecules. Low- and high-resolution STM images of the molecular adlayers on HOPG are shown in Fig. 2. In the large-scale STM image (Fig. 3*A*) the molecular network extends over the atomically flat terrace of the HOPG as a single domain over an area of 100 × 100 nm$^2$ without molecular defects. A careful observation of the low-resolution STM image (Fig. 2*A*) shows that the molecular adlayer is composed of bright lines along direction A and wide bands in direction B. The lines and bands intersect with an angle of 90 ± 2°. From the periodicity of the molecular self-organization, a unit cell with parameters of $a$ = 4.0 ± 0.2 nm (in the A direction), $b$ = 1.0 ± 0.2 nm (in the B direction), and an angle of 90°±2° can be discerned (Fig. 2).

A structural model for the self-organized adlayer is proposed in Fig. 2*C*. As observed in the high-resolution STM image (Fig. 2*B*), the basic unit constituting the adlayer appears as bright lines. The lines are parallel to direction A and are 3.1 ± 0.2 nm long. When viewed along direction B, the neighboring lines are interdigitated and form a close-packed arrangement. The distance, $d$, between two bright lines, when viewed along the B direction, is 1.2 ± 0.1 nm (Fig. 2*B*). The maximum corrugation height was determined to be 0.1 nm; however, this measure of the charge density cannot be considered a direct measure of the molecular thickness (Fig. 5, which is published as supporting information on the PNAS web

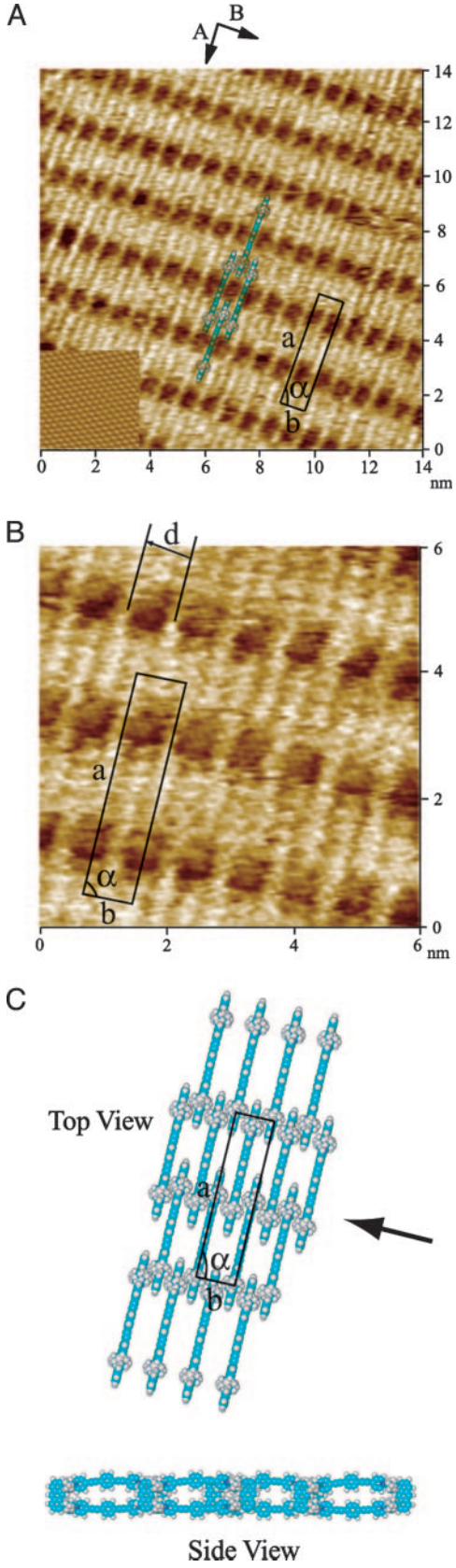


**Fig. 2.** STM images and structural model of the rectangle on HOPG. (*A*) Low-resolution image ($V_{bias}$ = 758 mV, $I_{tip}$ = 684 pA) showing a STM image of HOPG in the lower left corner. (*B*) High-resolution image ($V_{bias}$ = 876 mV, $I_{tip}$ = 691 pA. (*C*) A proposed structural model for the adlayer of the rectangle on HOPG surface.

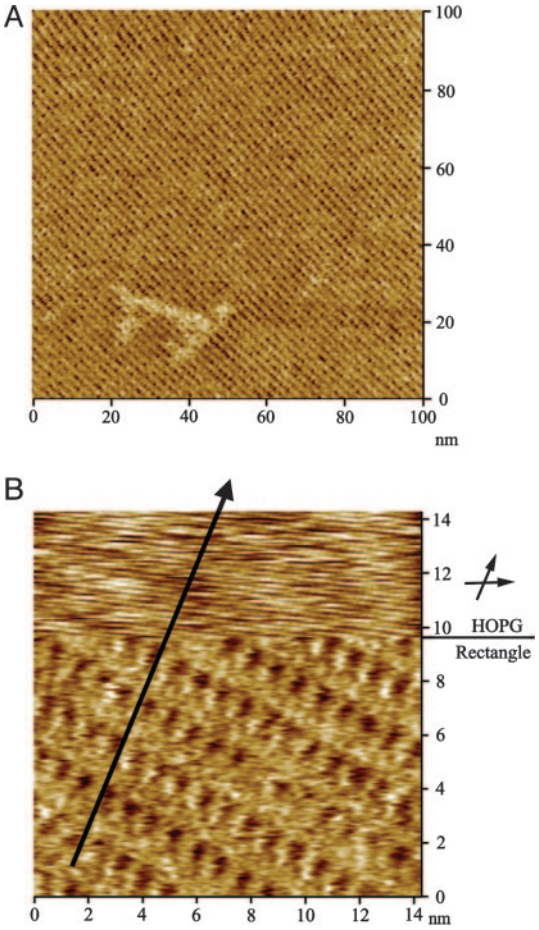


**Fig. 3.** STM images of the molecular rectangles on a HOPG substrate. (*A*) A large-scale (100 × 100 nm) STM image ($V_{bias}$ = 859 mV, $I_{tip}$ = 667 pA) of the rectangle adlayer. (*B*) A composite STM image showing the underlying HOPG lattice and the rectangle adlayer simultaneously. The imaging conditions are $V_{bias}$ = 859 mV, $I_{tip}$ = 667 pA for the molecular adlayer (*Lower*) and $V_{bias}$ = 15 mV, $I_{tip}$ = 667 pA for HOPG lattice (*Upper*).

site). The size of these lines is consistent with the dimension of the rectangle, as determined from the previously reported x-ray crystallographic data (28). Therefore, one bright line corresponds to a single rectangle standing vertically with its long edge standing on the underlying HOPG surface. A structural model for the self-organization of the rectangle on HOPG is proposed in Fig. 2*C* and superimposed in Fig. 2*A*. The proposed model is in good agreement with the observed STM images.

The adsorbed rectangles were found to be aligned along the underlying lattice of the HOPG. Fig. 3*B* is a composite STM image showing the orientation relation between the molecular adlayer and HOPG substrate. The image was recorded by jumping the bias during the STM scanning from the bottom to the upper frame. Although some image drifting occurs in the jumping, both the molecular adlayer and HOPG lattice are clearly observed in the composite image. The upper part of the frame shows the atomic resolution of the HOPG substrate, and the lower part shows the rectangle adlayer. The line crossing the two parts of the image indicates one direction of the HOPG lattice, indicated by the arrows in Fig. 3*B*. From the composite image, the crystal relationship between HOPG and the molecular adlayer can be directly deduced. The molecular rectangles form a close-packed arrangement on the HOPG surface, with the long edge of the rectangle oriented along the HOPG lattice.

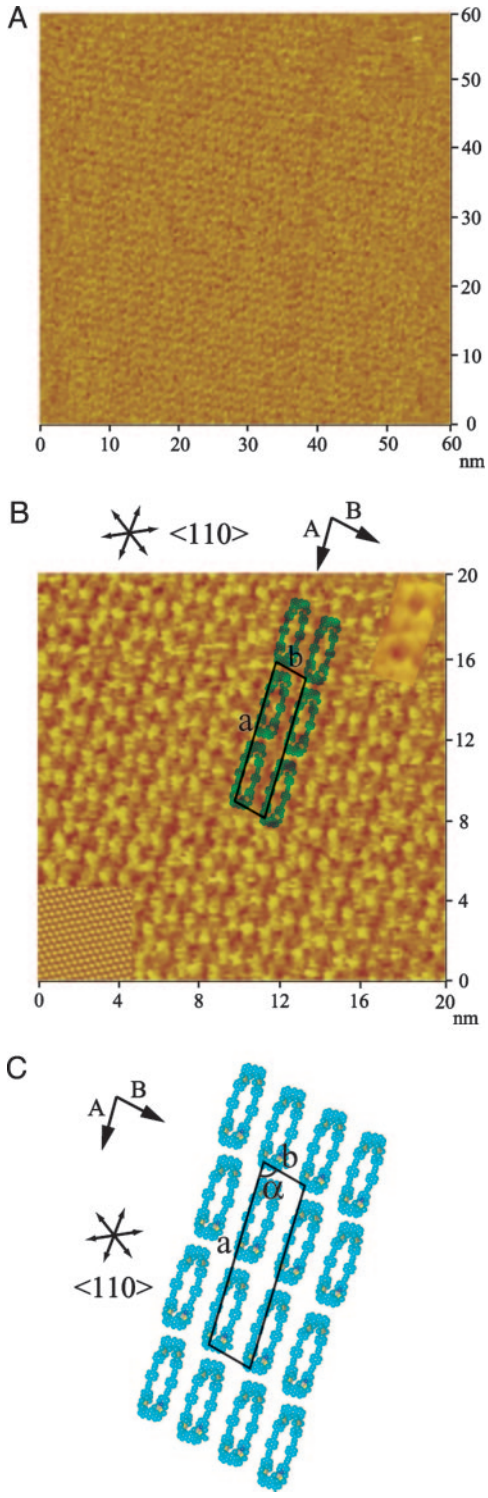


**Fig. 4.** STM images and structural model of the molecular rectangles on Au(111). (*A*) A large-scale (60 × 60 nm) image ($V_{bias}$ = −50 mV, $I_{tip}$ = 1.883 nA) of the rectangle adlayer. (*B*) High-resolution image ($V_{bias}$ = −50 mV, $I_{tip}$ = 1.698 nA) of the rectangle adlayer, showing the underlying Au(111) lattice in the lower left corner, and an individual rectangle is shown in the upper right corner. (*C*) A proposed structural model for the adlayer of the rectangle on Au(111) surface. STM images were recorded in 0.1 M $HClO_4$.

**Self-Organization on a Au(111) Surface.** It is well known that substrate can affect the self-organization of adsorbates (5–7). To determine how substrate affects absorption of the rectangle onto

surfaces, the molecular adlayer on Au(111), a widely used surface in nanodevice development, was also investigated. As observed on HOPG, immersion time (3 min) and solution concentration is critical to forming a monolayer on the Au(111) surface. When the gold bead is immersed in a $10^{-6}$ M solution of the rectangle, a uniform molecular adlayer is observed with very few defects (Fig. 4). Lower concentrations resulted in incomplete coverage of the Au(111) surface. At higher concentrations molecular clusters were observed in the STM images (Fig. 6, which is published as supporting information on the PNAS web site).

Bright rows of rectangles are observed along direction A in the high-resolution STM image (Fig. 4*B*). These images were recorded at 420 mV in 0.1 M $HClO_4$; however, the same adlayer was observed when the images were recorded in air (Fig. 7, which is published as supporting information on the PNAS web site). To understand the relationship between the adlayer and underlying substrate, the Au(111) surface was also imaged. After imaging the molecular adlayer, the Au(111) potential was scanned in the negative direction, resulting in desorption of the adsorbed rectangle. Thus, the Au(111)–$(1 \times 1)$ structure was resolved and is shown in the lower left corner of Fig. 4*B*. The hexagonal structure of the fcc(111) lattice can be seen in the Au(111). Each bright spot corresponds to one Au atom, and the interatomic distance is $0.28 \pm 0.2$ nm, consistent with the crystal parameter. A set of arrows indicate the <110> directions of the underlying Au(111) lattice. Compared with the underlying Au(111) substrate the molecular rows in the A direction are parallel to the <110> direction. As discussed above the molecules align along a lattice direction on the HOPG surface, and the same behavior is observed on the Au(111) surface.

Although molecular rows are visible, it is not easy to distinguish individual molecules in Fig. 4*B*. However, separated individual molecules or molecules in 1D ordering could be found on the Au(111) surface and were used to image an individual molecule. A rectangle with dark depressions in the center was observed, corresponding to a typical high-resolution STM image of a single molecule (Fig. 4*B*, upper right corner). The molecular size of the rectangle was determined to be $3.0 \pm 0.2$ by $1.1 \pm 0.2$ nm, consistent with the size of the rectangle determined from the x-ray crystallographic data (28). From the intermolecular distance and adlayer symmetry, a unit cell was determined. On the 2D surface one molecular row aligns along the A direction, and the periodic distance, $a$, is $8.3 \pm 0.2$ nm. A second molecular row goes along the B direction, and the distance between the neighboring molecules is $2.0 \pm 0.2$ nm. The A and B directions cross each other at an angle of $78 \pm 2°$. The proposed unit cell is shown in Fig. 4*B*; however, the exact boundary of an individual molecule is not clear. The proposed structural model is shown in Fig. 4*C*, where each molecule preserves its rectangular shape. The rectangle lays flat on the Au(111) surface, forming a well ordered self-organized pattern.

Self-organized adlayers are governed by intermolecular and molecular–substrate interactions. The interaction between molecule and substrate on the HOPG surface is weaker than that on the Au(111) surface. Therefore, the self-assembly on HOPG is dominated by intermolecular forces, resulting in a close-packed 2D molecular network. On the other hand, when the molecules adsorb on the Au(111) surface, only linear chains of rectangle molecules can be seen, likely caused by the stronger interactions between the rectangle molecules and the substrate. Although the molecules align along the two underlying lattices on both substrates, the actual structures on HOPG and Au(111) are completely different. Furthermore, the orientation of the adsorbed molecules, with respect to the substrate surface, depends on the substrate.

In summary, we have successfully prepared well ordered self-organized adlayers of nanoscopic metallacyclic molecular rectangles on HOPG and Au(111) surfaces. STM results show the adlayer symmetry and molecular arrangement of the rectangle on both surfaces. The rectangle is clearly observed with dark depressions in the center. Because of the difference in substrate materials, the long edge of the rectangles sits on the HOPG surface, and it lays flat on the Au(111) surface. Hence the molecular self-organization of the supramolecular metallacyclic rectangle on solid surfaces can be tuned by the appropriate choice of substrate materials. The defined conformation of the molecules with special properties will be significant for the fabrication of surface nanodevices.

L.-J.W. and C.-L.B. thank the National Natural Science Foundation of China (Grants 20025308, 20177025, 10028408, and 20121301), the National Key Project on Basic Research (Grant G2000077501), and the Chinese Academy of Sciences for financial support. P.J.S. thanks the National Institutes of Health (Grant GM-57052) and the National Science Foundation (Grant CHE-0306720) for financial support.

1. Lehn, J.-M. (2002) *Proc. Natl. Acad. Sci. USA* **99,** 4763–4768.
2. Whitesides, G. M. & Boncheva, M. (2002) *Proc. Natl. Acad. Sci. USA* **99,** 4769–4774.
3. Scudiero, L., Barlow, D. E., Mazur, U. & Hipps, K. W. (2001) *J. Am. Chem. Soc.* **123,** 4073–4080.
4. Hipps, K. W., Scudiero, L., Barclow, D. E. & Cooke, M. P., Jr. (2002) *J. Am. Chem. Soc.* **124,** 2126–2127.
5. Yoshimoto, S., Suto, K., Tada, A., Kobayashi, N. & Itaya, K. (2004) *J. Am. Chem. Soc.* **126,** 8020–8027.
6. Yoshimoto, S., Higa, N. & Itaya, K. (2004) *J. Am. Chem. Soc.* **126,** 8540–8545.
7. Barth, J. V., Weckesser, J., Cai, C., Günter, P., Bürgi, L., Jeandupeux, O. & Kern, K. (2000) *Angew. Chem. Int. Ed. Engl.* **39,** 1230–1234.
8. He, Y., Ye, T. & Borguet, E. (2002) *J. Am. Chem. Soc.* **124,** 11964–11970.
9. Xu, S., Szymanski, G. & Lipkowski, J. (2004) *J. Am. Chem. Soc.* **126,** 12276–12277.
10. Pan, G.-B., Liu, J.-M., Zhang, H.-M., Wan, L.-J., Zheng, Q.-Y. & Bai, C.-L. (2003) *Angew. Chem. Int. Ed. Engl.* **42,** 2747–2751.
11. Gong, J.-R., Lei, S.-B., Wan, L.-J., Deng, G.-J., Fan, Q.-H. & Bai, C.-L. (2003) *Chem. Mater.* **15,** 3098–3104.
12. Feyter, S. D., Abdel-Mottaleb, M. M. S., Schuurmans, N., Verkuijl, B. J. V., van Esch, J. H., Feringa, B. L. & Schryver, F. C. D. (2004) *Chem. Eur. J.* **10,** 1124–1132.
13. Semenov, A., Spatz, J. P., Möller, M., Lehn, J.-M., Sell, B., Schubert, D., Weidl, C. H. & Schubert, U. S. (1999) *Angew. Chem. Int. Ed. Engl.* **38,** 2547–2550.
14. Schwab, P. F. H., Levin, M. D. & Michl, J. (1999) *Chem. Rev.* **99,** 1863–1933.
15. Seidel, S. R. & Stang, P. J. (2002) *Acc. Chem. Res.* **35,** 972–983.
16. Holliday, B. J. & Mirkin, C. A. (2001) *Angew. Chem. Int. Ed. Engl.* **40,** 2022–2043.
17. Cotton, F. A., Lin, C. & Murillo, C. A. (2001) *Acc. Chem. Res.* **34,** 759–771.
18. Leininger, S., Olenyuk, B. & Stang, P. J. (2000) *Chem. Rev.* **100,** 853–908.
19. Caulder, D. L. & Raymond, K. N. (1999) *Acc. Chem. Res.* **32,** 975–982.
20. Fujita, M. (1998) *Chem. Soc. Rev.* **27,** 417–425.
21. Stang, P. J. & Olenyuk, B. (1997) *Acc. Chem. Res.* **30,** 502–518.
22. Cotton, F. A., Lin, C. & Murillo, C. A. (2002) *Proc. Natl. Acad. Sci. USA* **99,** 4810–4813.
23. Eddaoudi, M., Kim, J., Vodak, D., Sudik, A., Wachter, J., O'Keffe, M. & Yaghi, O. M. (2002) *Proc. Natl. Acad. Sci. USA* **99,** 4900–4904.
24. Pirondini, L., Bertolini, F., Cantadori, B., Ugozzoli, F., Massera, C. & Dalcanale, E. (2002) *Proc. Natl. Acad. Sci. USA* **99,** 4911–4915.
25. Kuehl, C. J., Kryschenko, Y. K., Radhakirshnan, U., Seidel, S. R., Huang, S. D. & Stang, P. J. (2002) *Proc. Natl. Acad. Sci. USA* **99,** 4932–4936.
26. Dinolfo, P. H. & Hupp, J. T. (2001) *Chem. Mater.* **13,** 3113–3125.
27. Würthner, F., You, C.-C. & Saha-Möller, C. R. (2004) *Chem. Soc. Rev.* **33,** 133–146.
28. Kuehl, C. J., Huang, S. D. & Stang, P. J. (2001) *J. Am. Chem. Soc.* **123,** 9634–9641.